Slovak University of Technology in Bratislava
Faculty of Civil Engineering

Ing. Viera Kleinová

Dissertation Thesis Abstract

Optical flow and its application for image processing

to obtain the Academic Title of *philosophiae doctor (PhD.)*
in the doctorate degree study programme
9.1.9 Applied Mathematics

Bratislava 2018

Dissertation Thesis has been prepared at Department of Mathematics and Descriptive Geometry, Faculty of Civil Engineering, Slovak University of Technology in Bratislava.

Submitter: Ing. Viera Kleinová
Department of Mathematics and Descriptive Geometry
Faculty of Civil Engineering, STU, Bratislava

Supervisor: doc. RNDr. Peter Frolkovič, PhD.
Department of Mathematics and Descriptive Geometry
Faculty of Civil Engineering, STU, Bratislava

Readers: prof. RNDr. Michal Fečkan, DrSc.
Department of Mathematical Analysis and Numerical Mathematics
FMFI UK, Bratislava

doc. Mgr. Ivan Cimrák, PhD.
Department of Software Technologies
FRI UNIZA, Žilina

RNDr. Ján Glasa, PhD.
Institute of Informatics
SAV, Bratislava

Dissertation Thesis Abstract was sent ....

Dissertation Thesis Defence will be held on .... at .... am/pm at Department of Mathematics and Descriptive Geometry, Faculty of Civil Engineering, Slovak University of Technology in Bratislava, Radlinského 11.

prof. Ing. Stanislav Unčík, PhD.
Dean of Faculty of Civil Engineering

Abstrakt

V práci opisujeme dve numerické metódy na odhad optického toku z dvoch po sebe nasledujúcich obrazov vo videosekvencii. Obe metódy sú založené na rovnici advekcie a hlavný rozdiel medzi metódami je v pridaných podmienkach na vektorové pole v rovnici advekcie. Pri riešení rovnice advekcie používame metódu charakteristík a optický tok získame použitím spätného sledovania charakteristík. Hlavným výsledkom práce je nová metóda na numerické riešenie rovnice advekcie pre pohyb v smere normály pomocou bilineárnej interpolácie, ktorá je vhodná pre odhad optického toku medzi obrazmi. V numerickej časti práce prezentujeme výsledky oboch metód, ktoré sme získali použitím 2D dát. Metódy sme testovali na dátach s presným riešením a použili sme ich aj pri odhade optického toku v reálnych dátach.

Kľúčové slová: optický tok, rovnica advekcie, charakteristické krivky, metóda spätného sledovania

Abstract

In this work we describe two numerical methods for optical flow estimation between two consecutive images in a video sequence. Both methods are based on the advection equation and the difference is on the choice of additional constraints for the velocity vector field. For solving the advection equation the characteristic curves are used and the optical flow is obtained using the backward tracking method to approximate the characteristics. The main results of this work is a new method for the numerical solution of advection equation for the motion in normal direction that is suitable for the optical flow estimation between images. We present numerical experiments on 2D synthetic data with exact solutions and on two dimensional real data.

Keywords: optical flow, advection equation, characteristic curves, backward tracking method

Contents

1   Introduction

Optical flow is an important topic in medicine, computer vision and image processing [1, 3, 5–7, 12]. It is a technique that is used to describe a deformation between images of a video sequence. The algorithms of optical flow estimation studied in this work are based on searching a deformation of one image toward the second one.

There are many methods that are dealing with the estimation of optical flow and the most popular ones are so-called differential methods [1, 6, 7, 12] as they are based on spatial derivatives of images.

Let the image sequence be described by a function $f = f(\mathbf{x}, t)$ defined on a domain $\mathbf{x} \in \Omega \subset \mathrm{R}^2$ where $\mathbf{x} = (x, y)$ denotes the location and $t \in [0, T]$ is the time. In such way the particular images are obtained for discrete values of t, e.g. $t = 0, 1, 2$ and so on. The methods of optical flow estimation describe in this work are based on the *advection equation* in the form

$$\partial_t f(\mathbf{x}, t) + u(\mathbf{x}, t) \partial_x f(\mathbf{x}, t) + v(\mathbf{x}, t) \partial_y f(\mathbf{x}, t) = 0, \tag{1.1}$$

where $\vec{u} = \vec{u}(\mathbf{x}, t) = (u, v) = (u(\mathbf{x}, t), v(\mathbf{x}, t))$ is the deformation and the subscripts denote the partial derivatives. In optical flow estimation the function f in (1.1) is considered to be known and the deformation $\vec{u}$ has to be determined.

If a method of optical flow is estimating the deformation $\vec{u}$ having a general vectorial form, the problem is typically underdefined. It means that the solution of formulated problem needs not to be unique. Therefore, some additional conditions are typically imposed on the estimated deformation $\vec{u}$ to formulate a problem with an unique solution.

In our work we describe two approaches for the estimation of the optical flow. Both approaches are based on the advection equation (1.1) and a backward tracking of characteristics. The first approach we are interested in is derived from the mathematical model created by Lucas and Kanade [7]. We use the idea of this method but in numerical implementation we modify it by suggesting a natural control of so-called CFL (Courant-Friedrichs-Lewy) [10].

The second approach is based on the level set formulation [8] and it is directly motivated by the model described in Sapiro et al. [1] and Vemuri et al. [12] that is slightly modified. We propose here a new numerical method of optical flow estimation. The new proposed numerical scheme is explicit, it means the numerical solution in one time step is defined directly and no linear system of equations must be solved.

This work is organized as follows. Chapter 2 contains the mathematical formulation of the advection equation and its solution. We introduce the mathematical models of the Lucas and Kanade method and the method based on the level set motion. In Chapter 3 we describe the numerical implementation of backward tracking method and we propose the numerical implementation of both methods. Chapter 4 includes numerical experiment on synthetic data with exact solution. Finally, conclusions and further research can be found in Chapter 5.

2 Mathematical model

In this chapter we describe the mathematical formulation of optical flow based on advection equation and its solution using characteristic curves. The method of Lucas and Kanade and the method based on level set motion are described in this chapter.

2.1 The optical flow estimation

Let F and G be a given two-dimensional functions e.g. the functions of the intensity of grayscale images. The functions $F = F(\mathbf{x})$ and $G = G(\mathbf{x})$ are defined on a domain $\Omega \subset \mathrm{R}^2$ for $\mathbf{x} \in \Omega$. The main aim of optical flow estimation is to find a deformation $\vec{U}$ under which the function F is transferred to the function G. As we define later this can be described by a vector function $\vec{U} = \vec{U}(\mathbf{x})$ such that

$$F(\mathbf{x} - \vec{U}(\mathbf{x})) = G(\mathbf{x}). \tag{2.1}$$

The solution of this problem does not seem to be complicated, but the opposite is true. The solution of the optical flow estimation is nontrivial because different situations can occur, e.g. the optical flow does not exist (see Fig. 1) or there are many optical flows (see Fig. 2).

Therefore, some additional constraints are typically imposed on the estimate of $\vec{U}$ to formulate a problem with an unique solution. In our work we consider two methods with different additional constraints on $\vec{U}$ for the optical flow estimation. The first one is based on minimization of function and the second one is based on level set motion. The both approaches are related to the advection equation that we introduce in the next section.
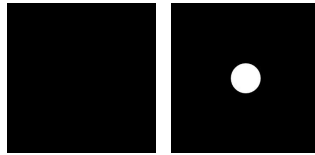

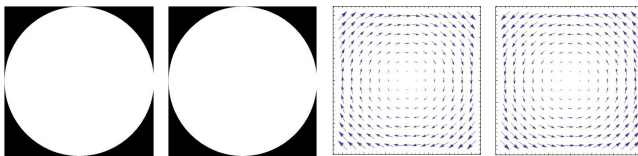Figure 1: The optical flow does not exist. From the left to the right: the function F, the function G.

Figure 2: There are many optical flows. From the left to the right: the function F, the function G, rotation in the clockwise direction, rotation in the counter-clockwise direction.

2.2 The advection equation

The basic idea of our approach in this work is to search for a function $f = f(\mathbf{x}, t)$ that fulfils the advection equation (1.1), i.e.

$$\partial_t f(\mathbf{x}, t) + \vec{u}(\mathbf{x}, t) \cdot \nabla f(\mathbf{x}, t) = 0, \qquad f(\mathbf{x}, 0) = F(\mathbf{x}). \tag{2.2}$$

Our aim is to define $\vec{u}$ such that $f(\mathbf{x}, T) = G(x)$ where $T > 0$ is not yet specified time. The notation $\nabla f(\mathbf{x}, t) = (\partial_x f(\mathbf{x}, t), \partial_y f(\mathbf{x}, t))$ is the spatial gradient of function.

2.3 The method of characteristics

For solving the advection equation in the form (2.2), the method of characteristics can be used. Let $\vec{u}$ in (2.2) be known, then the *characteristic curves* $X = X(\mathbf{x}, \tilde{t}; t)$ for some $\tilde{t} \in [0, T]$ and $\mathbf{x} \in \Omega$ are the solutions of ordinary differential equations

$$\dot{X}(\mathbf{x}, \tilde{t}; t) = \vec{u}(X(\mathbf{x}, \tilde{t}; t), t), \qquad X(x, \tilde{t}; \tilde{t}) = \mathbf{x}. \tag{2.3}$$

The value $X(\mathbf{x}, \tilde{t}; t)$ denotes the position X of characteristic curve at time t for which the position at time $\tilde{t}$ is $\mathbf{x}$.

For the solution $f(\mathbf{x}, t)$ of (2.2) we see that the time derivative of $f(X(\mathbf{x}, \tilde{t}; t), t)$ vanishes along $X(\mathbf{x}, \tilde{t}; t)$

$$\begin{aligned}
\frac{\mathrm{d}}{\mathrm{d}t} f(X(\mathbf{x}, \tilde{t}; t), t) &= \partial_t f(X(\mathbf{x}, \tilde{t}; t), t) + \dot{X}(\mathbf{x}, \tilde{t}; t) \cdot \nabla f(X(\mathbf{x}, \tilde{t}; t), t) \\
&= \partial_t f(X(\mathbf{x}, \tilde{t}; t), t) + \vec{u}(X(\mathbf{x}, \tilde{t}; t), t) \cdot \nabla f(X(\mathbf{x}, \tilde{t}; t), t) \\
&= 0,
\end{aligned} \tag{2.4}$$

if all derivatives exist. We can conclude that the function f is constant along the characteristic curves.

In our work we consider so-called *backward tracking of characteristics* for $\mathbf{x} \in \Omega$ from $t = \tilde{t} = T$ to $t = 0$ in the form

$$\dot{X}(\mathbf{x}, T; t) = \vec{u}(X(\mathbf{x}, T; t), t), \qquad X(\mathbf{x}, T; T) = \mathbf{x}. \tag{2.5}$$

Let f be a smooth solution of the advection equation (2.2) such that $f(\mathbf{x}, T) = G(\mathbf{x})$ for $\mathbf{x} \in \Omega$, we obtained

$$\begin{aligned}
F(X(\mathbf{x}, T; 0)) &= f(X(\mathbf{x}, T; 0), 0) = f(X(\mathbf{x}, T; t), t) = f(X(\mathbf{x}, T; T), T) \\
&= f(\mathbf{x}, T) = G(\mathbf{x}),
\end{aligned} \tag{2.6}$$

so we can define the deformation $\vec{U}$ as follows

$$\vec{U}(\mathbf{x}) = \mathbf{x} - X(\mathbf{x}, T; 0). \tag{2.7}$$

There are several methods how to solve the advection equation (2.2) numerically when $\vec{u}$ is given. We search for a numerical approximation of the function $f(\mathbf{x}, \tilde{t})$ by

using the property (2.4), i.e.

$$f(\mathbf{x}, \tilde{t}) = F(X(\mathbf{x}, \tilde{t}; 0)), \tag{2.8}$$

where to obtain $X(\mathbf{x}, \tilde{t}; 0)$ in (2.8) we solve (2.3) numerically.

2.4 Lucas and Kanade method

The Lucas and Kanade [7] method assumes that the optical flow is constant within some local neighbourhood of the location $\mathbf{x} \in \Omega$. The method is used mostly to find a small and approximately constant geometric deformation. The required additional constraints on $\vec{u}$ are obtained by a minimization of some appropriate function.

For determining $\vec{u}$ for each $\mathbf{x} \in \Omega$ and $t \in [0, T]$ we minimize the function

$$E_{LK}(u, v) = K_\sigma * \left((\Delta_t f + u \partial_x f + v \partial_y f)^2 \right), \tag{2.9}$$

where $\Delta_t f = (G - f)$ and $*$ denotes the convolution of the Gaussian function K_σ and $(\Delta_t f + u \partial_x f + v \partial_y f)^2$.

Consequently, we can determine u and v at some location $\mathbf{x} \in \Omega$ and at time t by using a necessary condition for the minimum of E_{LK} in (2.9) that is reached if $\partial_u E_{LK}(u, v) = 0$ and $\partial_v E_{LK}(u, v) = 0$, i.e.

$$\begin{aligned} K_\sigma * [2(\partial_x f u + \partial_y f v + \Delta_t f) \partial_x f] &= 0, \\ K_\sigma * [2(\partial_x f u + \partial_y f v + \Delta_t f) \partial_y f] &= 0. \end{aligned} \tag{2.10}$$

The solution of this minimization problem (2.10) can be obtained from the linear system in the form

$$\begin{pmatrix} K_\sigma * (\partial_x f)^2 & K_\sigma * (\partial_x f \partial_y f) \\ K_\sigma * (\partial_y f \partial_x f) & K_\sigma * (\partial_y f)^2 \end{pmatrix} \begin{pmatrix} u \\ v \end{pmatrix} = \begin{pmatrix} -K_\sigma * (\partial_x f \Delta_t f) \\ -K_\sigma * (\partial_y f \Delta_t f) \end{pmatrix}. \tag{2.11}$$

Consequently, to determine the evolving function f one has to solve the advection equation (2.2) coupled with the additional equations (2.11) for $\vec{u}$.

2.5 Method based on level set motion

This approach is based on the mathematical models proposed by Sapiro et al. [1] and Vemuri et al. [12]. It is based on level-set formulation and the additional required constraints for $\vec{u}$ are obtained by restricting the optical flow only in normal directions to the level sets of the evolving function f.

Our aim in this method is to evolve the function f from F toward the function G by prescribing the motion only in normal direction. In this case we consider $\vec{u}$ in the advection equation (2.2) of the form

$$\vec{u} = \begin{cases} -\operatorname{sgn}(G - f) \frac{\nabla f}{|\nabla f|} & |\nabla f| \neq 0, \\ \vec{0} & |\nabla f| = 0. \end{cases} \tag{2.12}$$

where sgn is the standard sign function, it means that

$$\text{sgn}(p) = \begin{cases} -1 & p < 0, \\ 0 & p = 0, \\ 1 & p > 0, \end{cases} \tag{2.13}$$

where p is a real number. The vector field $\vec{u}$ for $|\nabla f| \neq 0$ represents the normal vectors to level sets of f. The orientation of the normal vectors are given by $\text{sgn}(G - f)$.

Note that the equation (2.2) can be rewritten into the level set equation

$$\partial_t f = \text{sgn}(G - f)|\nabla f|. \tag{2.14}$$

The level set equation (2.14) describes the movement of level sets of the function f in normal direction. If $\nabla f(\mathbf{x}, t) \neq \vec{0}$ then the speed in normal direction is 1 if $f(\mathbf{x}, t) > G(\mathbf{x})$ or -1 if $f(\mathbf{x}, t) < G(x)$. It can change to 0 if $f = G$ or $\nabla f = \vec{0}$ that must be taken into consideration in numerical methods. We note that by setting the normal component of ∇f to zero at boundary $\partial\Omega$ of the domain Ω we define the boundary conditions for the advection equation (2.2).

The level set equation (2.14) can be solved directly for the function f. The vector function $\vec{u}$ can be determined from (2.12) afterwards. Once the function $\vec{u}$ is known, we can compute the characteristic curves using the backward tracking method (2.5).

3 Numerical models

In this chapter we start with the discretization of the given domain and the functions and the implementation of backward tracking method. In detail we present the numerical implementations of the Lucas and Kanade method defined in Section 2.4 and the method based on level-set motion defined in Section 2.5.

3.1 Discretization of the domain and the functions

We create a uniform grid with the centres $\mathbf{x}_{ij} = (x_i, y_j) := (ih, jh)$ where $i = 0, \ldots, I-1$ and $j = 0, \ldots, J-1$ are the coordinates and $h > 0$ is a discretization step. We suppose that the functions $F(\mathbf{x})$ and $G(\mathbf{x})$ for $\mathbf{x}$ are obtained by standard bilinear interpolation of given discrete values $F_{ij} = F(\mathbf{x}_{ij})$ and $G_{ij} = G(\mathbf{x}_{ij})$. The main goal of this work is to find a numerical approximation of deformation $\vec{U}(\mathbf{x})$ represented by discrete values $\vec{U}_{ij} \approx \vec{U}(\mathbf{x}_{ij})$ such that $G_{ij} \approx F(\mathbf{x}_{ij} - \vec{U}_{ij})$. The positions $\mathbf{x}_{ij} - \vec{U}_{ij}$ rarely coincide with the positions of points, therefore the values $F(\mathbf{x}_{ij} - \vec{U}_{ij})$ are obtained by using the bilinear interpolation.

The bilinear interpolation is a method that uses the distance weighted average of the four nearest values to estimate a new value (see Fig. 3). Let $d_{ij} = d(\mathbf{x}_{ij})$ be the known discrete values of function d. To compute $d(\mathbf{x})$ for any $\mathbf{x}$ we use the bilinear interpolation. We compute $i = \lfloor \frac{x}{h} \rfloor$, $j = \lfloor \frac{y}{h} \rfloor$, $t_i = \frac{x}{h} - i$, $t_j = \frac{y}{h} - j$ where $\lfloor \cdot \rfloor$ is the floor

6

function. Of course we require that $0 \leq i \leq I-1$ and $0 \leq j \leq J-1$. To define the value $d(\mathbf{x})$ by the bilinear interpolation we use the four known neighbouring values d_{ij}, $d_{i+1\,j}$, $d_{i\,j+1}$, and $d_{i+1\,j+1}$, such that

$$d(\mathbf{x}) = (1-t_i)\left[(1-t_j)\,d_{ij} + t_j d_{i\,j+1}\right] + t_i\left[(1-t_j)\,d_{i+1\,j} + t_j d_{i+1\,j+1}\right]. \qquad (3.1)$$
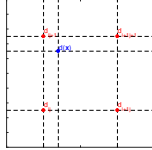

Figure 3: The bilinear interpolation.

3.2   Discretization of the backward tracking method

First, we discretize the time steps t^n. For simplicity the time steps are chosen to be $t^n = n\tau$ for $n = 0,\ldots,N$, where the choice of N is described later in this section. The choice of τ is different for each method and it will be presented in sections on numerical implementations of the methods.

The characteristic curves are approximated by the discrete values $X_{ij}^{n,m} \approx X(\mathbf{x}_{ij}, t^n; t^m)$. We are interested only in the approximation of $X(\mathbf{x}_{ij}, t^n; 0)$ we propose the approximation of the form $X_{ij}^{n+1,0} = X(\mathbf{x}_{ij}, t^{n+1}; 0)$ given by

$$X_{ij}^{n+1,0} = X^{n,0}(x_{ij} - \tau \vec{u}_{ij}^n), \qquad X_{ij}^{0,0} = x_{ij}, \qquad (3.2)$$

where $X^{n+1,0}$ is the bilinear interpolation of values $X_{ij}^{n+1,0}$. Only one bilinear interpolation is used per each time steps.

Once the approximated characteristics are available we can approximate $f_{ij}^n \approx f(\mathbf{x}_{ij}, t^n)$ as in equation (2.8) by

$$f_{ij}^n = F(X_{ij}^{n,0}), \qquad (3.3)$$

for $n > 0$ and for $n = 0$ we set $f_{ij}^0 = F_{ij}$.

Now we can define the choice of N. The stopping time t^N is reached if an estimate of the distance between the functions f_{ij}^N and G_{ij} is small enough, such that $f_{ij}^N \approx G_{ij}$ for all indices i and j. For the method based on the level set motion the norm of the gradient of the function f_{ij}^N can be approximately zero that will be also considered for the choice of stopping time, see later.

Finally, when $n = N$ the discrete values $\vec{U}_{ij}$ of the proximate deformation between

two functions F_{ij} and G_{ij} is given by the approximation of (2.7) using (3.2)

$$\vec{U}_{ij} = \mathbf{x}_{ij} - X_{ij}^{N,0}. \tag{3.4}$$

3.3 Discretization of the advection equation

In this section we consider a numerical approximation of the advection equation (2.2) in the form

$$f_{ij}^{n+1} = f_{ij}^n - \tau \vec{u}_{ij}^n \cdot \nabla f_{ij}^n, \qquad f_{ij}^0 = F_{ij}, \tag{3.5}$$

where the choice of values $\vec{u}_{ij}^n = (u_{ij}^n, v_{ij}^n)$ will be defined for the Lucas and Kanade method and the method based on level set motion in next sections. Note that to compute the values f_{ij}^{n+1} we use the method (3.3) and not the method (3.5). The main purpose of this section is to define a control of time steps τ using (3.5). Moreover the approximations of gradients are introduced here.

In the case of the numerical approximation (3.5) of the advection equation (2.2) a restriction on the time step τ is available in the form of CFL (Courant-Friedrichs-Lewy) condition [10] for each time t^n, namely

$$\tau \leq \frac{h}{|u_{ij}^n| + |v_{ij}^n|}, \tag{3.6}$$

if $\vec{u}_{ij}^n \neq \vec{0}$. We use it later in next sections.

Furthermore, for an approximation of the gradient $\nabla f_{ij}^n \approx \nabla f(\mathbf{x}_{ij}, t^n)$ we introduce two types of approximation.

Firstly, the spatial derivatives $\partial_x f_{ij}^n$ and $\partial_y f_{ij}^n$ can be approximated by central finite differences

$$\begin{aligned} 2h\partial_x f_{ij}^n &= f_{i+1j}^n - f_{i-1j}^n, \\ 2h\partial_y f_{ij}^n &= f_{ij+1}^n - f_{ij-1}^n. \end{aligned} \tag{3.7}$$

On the boundary the forward and backward finite differences are used

$$\begin{aligned} h\partial_x f_{0j}^n &= f_{1j}^n - f_{0j}^n, \\ h\partial_x f_{I-1j}^n &= f_{I-1j}^n - f_{I-2j}^n, \\ h\partial_y f_{i0}^n &= f_{i1}^n - f_{i0}^n, \\ h\partial_y f_{iJ-1}^n &= f_{iJ-1}^n - f_{iJ-2}^n. \end{aligned} \tag{3.8}$$

The approximations of the gradient as defined in (3.7) and (3.8) will be used in the Lucas and Kanade method. Note that such approximation is not suitable to be used in (3.5).

The second type of approximation of the gradient is used for the method based on the level set motion. The gradient ∇f_{ij}^n is approximated by upwind scheme from [11] as

8

follows

$$
h\partial_x f_{ij}^n = \begin{cases} f_{ij}^n - f_{i-1j}^n & f_{i-1j}^n = \text{ext}\{f_{i-1j}^n, f_{ij}^n, f_{i+1j}^n\} \\ f_{i+1j}^n - f_{ij}^n & f_{i+1j}^n = \text{ext}\{f_{i-1j}^n, f_{ij}^n, f_{i+1j}^n\} \\ 0 & f_{ij}^n = \text{ext}\{f_{i-1j}^n, f_{ij}^n, f_{i+1j}^n\} \end{cases} \tag{3.9}
$$

$$
h\partial_y f_{ij}^n = \begin{cases} f_{ij}^n - f_{ij-1}^n & f_{ij-1}^n = \text{ext}\{f_{ij-1}^n, f_{ij}^n, f_{ij+1}^n\} \\ f_{ij+1}^n - f_{ij}^n & f_{ij+1}^n = \text{ext}\{f_{ij-1}^n, f_{ij}^n, f_{ij+1}^n\} \\ 0 & f_{ij}^n = \text{ext}\{f_{ij-1}^n, f_{ij}^n, f_{ij+1}^n\} \end{cases} \tag{3.10}
$$

where ext denotes the extreme values among the three disrete values of f_{ij}^n in (3.9) or (3.10) with the choice

$$
\text{ext} = \begin{cases} \min & (G_{ij} - f_{ij}^n) < 0 \\ \max & (G_{ij} - f_{ij}^n) > 0 \end{cases} \tag{3.11}
$$

We modify the definitions (3.9) and (3.10) on the boundary by simply skipping the discrete values of f outside of the computational domain.

3.4   Numerical implementation of Lucas and Kanade method

In this section we perform the discretization of Lucas and Kanade method defined in 2.4. The numerical implementation of this method is described in [3, 7]. In detail we present a slightly modified version of this method that we use later in our numerical experiments.

Let the values f_{ij}^n be known, in particular $f_{ij}^0 = F_{ij}$, then the linear system defined in (2.11) is approximated by

$$
\begin{pmatrix} W_\sigma * (\partial_x f_{ij}^n)^2 & W_\sigma * (\partial_x f_{ij}^n \partial_y f_{ij}^n) \\ W_\sigma * (\partial_y f_{ij}^n \partial_x f_{ij}^n) & W_\sigma * (\partial_y f_{ij}^n)^2 \end{pmatrix} \begin{pmatrix} u_{ij}^n \\ v_{ij}^n \end{pmatrix} = \begin{pmatrix} -W_\sigma * (\partial_x f_{ij}^n \Delta_t f_{ij}^n) \\ -W_\sigma * (\partial_y f_{ij}^n \Delta_t f_{ij}^n) \end{pmatrix}.
$$
$$\tag{3.12}$$

where W_σ represents a discrete form of Gaussian function K_σ. This linear system can be solved if the matrix in (3.12) is invertible. The matrix is invertible if a determinant of the matrix is nonzero. If this determinant is less than a regularization parameter ε_e, see later, then we set $\vec{u}_{ij}^n = \vec{0}$, otherwise we solve the system (3.12) to obtain $\vec{u}_{ij}^n$.

The spatial derivatives $\partial_x f_{ij}^n$ and $\partial_y f_{ij}^n$ are approximated by the central differences defined in (3.7) and (3.8).

Let $g(\mathbf{x}_{ij}, t)$ be a function than the discrete convolution of W_σ and the function g that approximates the integral convolution is given by

$$
W_\sigma * g(x_i, y_j, t^n) = \frac{1}{\sum_{k,l} w_{kl}} \sum_{k,l} w_{kl} f(x_i + kh, y_j + lh, t^n), \tag{3.13}
$$

where $-3\sigma < k < 3\sigma$ and $-3\sigma < l < 3\sigma$ and

$$w_{kl} = \frac{1}{2\pi\sigma^2} \exp^{-\frac{k^2+l^2}{2\sigma^2}}, \tag{3.14}$$

where σ is a standard deviation. In practice, to compute the discrete approximation of (3.13) the elements w_{ij} for $-3\sigma > k > 3\sigma$ and $-3\sigma > l > 3\sigma$ are neglected. In image processing programs the discrete Gaussian function is presented with a matrix of dimension $\lceil 6\sigma \rceil \times \lceil 6\sigma \rceil$, where $\lceil \cdot \rceil$ is the ceiling function.

In our numerical implementation of Gaussian function we choose the convolution matrix with a size $M \times M$, where M is an odd integer and the standard deviation σ is set to $M/6$. For the values outside of the area we use the reflection of these values. The dimension M determines the neighbourhood of each pixel for which the assumption about constant optical flow is considered. The choice of the size M of the convolution matrix is a non-trivial task.

The origin idea of Lucas Kanade method [7] is to apply no restrictions on the magnitude of the vector $\vec{u}_{ij}^n$. In [2], they use Gaussian pyramidal representation for estimating large deformation between images. In our work we use the CFL condition defined in (3.6). We propose to choose in each contribution $\tau\vec{u}_{ij}^n$ the maximal value for τ between 1 that corresponds to the origin Lucas Kanade method and a variable choice fulfilling the CFL condition. The simplest way is to define the variable time step τ_{ij}^n of the form

$$\tau_{ij}^n = \min\{1, \frac{h}{|u_{ij}^n| + |v_{ij}^n|}\}, \tag{3.15}$$

and (3.2) becomes

$$\tilde{X}_{ij}^{n+1,0} = \tilde{X}^{n,0}(x_{ij} - \tau_{ij}^n \vec{u}_{ij}^n), \qquad \tilde{X}_{ij}^{0,0} = x_{ij}. \tag{3.16}$$

Once the values u_{ij}^n and v_{ij}^n are found using (3.12) the characteristic curves $\tilde{X}_{ij}^{n,0}$ defined in (3.2) are used to determine new value f_{ij}^{n+1} by (3.3). When $n = N$ the optical flow estimation by $\vec{U}_{ij}$ between F and G is given by (3.4)

3.5 Numerical implementation of the method based on level set motion

In this section we present the numerical implementation of the method based on level set motion defined in Section 2.5.

First we consider a numerical approximation of the advection equation (3.5), where $\vec{u}_{ij}^n$ defined in (2.12) is approximated by

$$\vec{u}_{ij}^n = \begin{cases} -s_{ij}^n \frac{\nabla f_{ij}^n}{|\nabla f_{ij}^n|} & |\nabla f_{ij}^n| \neq 0 \\ \vec{0} & |\nabla f_{ij}^n| = 0. \end{cases} \tag{3.17}$$

Now the equation (3.5) can be rewritten using (3.17) in the form

$$f_{ij}^{n+1} = f_{ij}^n + \tau s_{ij} \frac{\nabla f_{ij}^n}{|\nabla f_{ij}^n|} \cdot \nabla f_{ij}^n, \tag{3.18}$$

if $|\nabla f_{ij}^n| \neq 0$ and s_{ij} is defined by

$$s_{ij} = \text{sgn}(G_{ij} - F_{ij}). \tag{3.19}$$

Note that if $f_{ij}^n = G_{ij}$ we require $f_{ij}^{n+k} \equiv f_{ij}^n$ for $k = 1, 2, \ldots$. We remind that the scheme (3.18) is introduced only to derive a control of time steps τ.

Let the values f_{ij}^n be known for some $n \geq 0$, e.g. $f_{ij}^0 = F_{ij}$. If $f_{ij}^n = G_{ij}$ we simply replace (3.19) by $s_{ij} = 0$. In what follows we suppose that $f_{ij}^n \neq G_{ij}$ and that $\text{sgn}(G_{ij} - f_{ij}^n) = \text{sgn}(G_{ij} - F_{ij}) = s_{ij}$.

We apply the Rouy-Tourin scheme [9, 11] to define the values f_{ij}^{n+1} in (3.17), where the approximation of ∇f_{ij}^n is given by (3.9) and (3.10). We rewrite the scheme (3.18) using the components of $\nabla f_{ij}^n = (\partial_x f_{ij}^n, \partial_y f_{ij}^n)$ into the form

$$f_{ij}^{n+1} = f_{ij}^n + \tau s_{ij} \left(\frac{\partial_x f_{ij}^n}{|\nabla f_{ij}^n|} \partial_x f_{ij}^n + \frac{\partial_y f_{ij}^n}{|\nabla f_{ij}^n|} \partial_y f_{ij}^n \right). \tag{3.20}$$

One can easily show that $h|\partial_x f_{ij}^n| = |f_{i+kj}^n - f_{ij}^n| = s_{ij}(f_{i+kj}^n - f_{ij}^n)$ and $h|\partial_y f_{ij}^n| = |f_{ij+l}^n - f_{ij}^n| = s_{ij}(f_{ij+l}^n - f_{ij}^n)$, where $k, l \in \{-1, 0, 1\}$ be such that the value f_{i+kj} is the extreme value chosen in (3.9) and the value f_{ij+l}^n is chosen in (3.10).

Furthmore, let

$$U_{ij}^n = \frac{\tau}{h} \frac{|\partial_x f_{ij}^n|}{|\nabla f_{ij}^n|}, \qquad V_{ij}^n = \frac{\tau}{h} \frac{|\partial_y f_{ij}^n|}{|\nabla f_{ij}^n|}, \tag{3.21}$$

so the scheme (3.20) can be written in the form

$$f_{ij}^{n+1} = (1 - U_{ij}^n - V_{ij}^n) f_{ij}^n + U_{ij}^n f_{i+kj}^n + V_{ij}^n f_{ij+l}^n. \tag{3.22}$$

The scheme (3.22) defines the new value f_{ij}^{n+1} as a convex combination of three values f_{ij}^n, f_{i+kj}^n and f_{ij+l}^n is the following restriction is fulfilled,

$$U_{ij}^n + V_{ij}^n \leq 1. \tag{3.23}$$

The sufficient condition for (3.23) is that $\tau \leq \frac{h}{\sqrt{2}}$ that follows from (3.21).

Note that the definition (3.22) corresponds to a linear interpolation of three values f_{ij}^n, f_{i+kj}^n and f_{ij+l}^n and that the "corner" value f_{i+kj+l}^n is not involved. As discussed in Section 3.1 one prefers the bilinear interpolation for data representing images which uses in general four discrete values of the interpolated function. For this reason we suggest another numerical scheme that is based on so called Corner Transport Upwind scheme

[4, 10] and that can be viewed as an extension of the scheme (3.22), namely

$$f_{ij}^{n+1} = (1 - U_{ij}^n - V_{ij}^n)f_{ij}^n + U_{ij}^n f_{i+kj}^n + V_{ij}^n f_{ij+l}^n + U_{ij}^n V_{ij}^n (f_{ij}^n - f_{i+kj}^n - f_{ij+l}^n + f_{i+kj+l}^n),$$
(3.24)

The scheme (3.24) defines the new value f_{ij}^{n+1} as a convex combination of four values f_{ij}^n, f_{i+kj}^n, f_{ij+l}^n and f_{i+kj+l}^n if

$$\max \left\{U_{ij}^n, V_{ij}^n\right\} \leq 1.$$
(3.25)

A sufficient condition to obtained (3.25) is to require that $\tau \leq h$. We see that this restriction for Corner Transport Upwind scheme is less restrictive than the restriction for Rouy-Tourin scheme defined in (3.23).

In what follows we derive particular choices of the time step τ in (3.24) for each index i and j. To do so using (3.21) we rewrite the equation (3.24) in the form

$$\tilde{f}_{ij}^{n+1}(\tau) = f_{ij}^n + \tau s_{ij}|\nabla f_{ij}^n| + \tau^2 \frac{d_{ij}^n}{|\nabla f_{ij}^n|^2},$$
(3.26)

where

$$d_{ij}^n := \frac{1}{h^2}|\partial_x f_{ij}^n \partial_y f_{ij}^n|\left(f_{ij}^n - f_{i+kj}^n - f_{ij+l}^n + f_{i+kj+l}^n\right).$$
(3.27)

Finally we can suggest a choice of the time step τ to be used in (3.26), respectively in (3.24). As $\tilde{f}_{ij}^{n+1}(\tau)$ is a quadratic function of τ, and $\frac{d}{d\tau}\tilde{f}_{ij}^{n+1}(0) = s_{ij}|\nabla f_{ij}^n|$, we can claim that if $|\nabla f_{ij}^n| \neq 0$ and $s_{ij} \neq 0$ then for enough small time step $\tau > 0$ one has that

$$|\tilde{f}_{ij}^{n+1}(\tau) - G_{ij}| < |f_{ij}^n - G_{ij}|.$$
(3.28)

This means that for a small enough time step the value $\tilde{f}_{ij}^{n+1}(\tau)$ will be closer to the value G_{ij} than the value f_{ij}^n that is, of course, the desired property.

Our aim is to use the maximal value $\tau = h$ to speed up the evolution of the values $\tilde{f}_{ij}^{n+1}$ towards the values G_{ij}. Nevertheless, there are two cases for this choice of τ when the scheme (3.26) has to be used with different time step. These two cases will be described formally by a variable choice of $\tau = \tau_{ij}^n$ in (3.26).

In the case 1 we want to avoid that $\text{sgn}(G_{ij} - \tilde{f}_{ij}^{n+1}(\tau)) \neq s_{ij}$ for $\tau = h$, where s_{ij} is defined in (3.19). If this happens there exists $\tau_{ij}^n < h$ such that $\tilde{f}_{ij}^{n+1}(\tau_{ij}^n) = G_{ij}$ that is, of course, the aim of our method. Therefore in the case 1 we use (3.26) with $\tau = \tau_{ij}^n$.

In the case 2 we want to avoid that there exists some $\tau_{ij}^n < h$ when the derivative $\frac{d}{d\tau}\tilde{f}_{ij}^{n+1}(\tau_{ij}^n)$ vanishes. The reason is that for such situation one has for $\tau > \tau_{ij}^n$ that $|\tilde{f}_{ij}^{n+1}(\tau) - G_{ij}| > |\tilde{f}_{ij}^{n+1}(\tau_{ij}^n) - G_{ij}|$, and, such property is not desired. Therefore in the case 2 we use again $\tau = \tau_{ij}^n$.

Consequently, in both cases we should use the scheme (3.26) with the variable time steps $\tau = \tau_{ij}^n$, otherwise we can take the maximal time step $\tau = h$.

In what follows we define the variable time steps τ_{ij}^n in detail that will be used in

(3.26). To do so we suppose that $|\nabla f_{ij}^n| \neq 0$ and $f_{ij}^n \neq G_{ij}$. We need to distinguish three situations.

Firstly, if $d_{ij}^n = 0$ then $\tilde{f}_{ij}^{n+1}(\tau)$ becomes a linear function. To control the case 1 and to follow the restriction of maximal time step we require in the first situation that

$$\tau_{ij}^n = \min\{h, \frac{|G_{ij} - f_{ij}^n|}{|\nabla f_{ij}^n|}\}. \tag{3.29}$$

Furthermore let $d_{ij}^n \neq 0$. To control the case 1 and the case 2 we search for such τ that

$$G_{ij} = f_{ij}^n + \tau s_{ij} |\nabla f_{ij}^n| + \tau^2 \frac{d_{ij}^n}{|\nabla f_{ij}^n|^2}. \tag{3.30}$$

and $\frac{d}{d\tau} \tilde{f}_{ij}^{n+1}(\tau) = 0$, it means

$$s_{ij} |\nabla f_{ij}^n| + 2\tau \frac{d_{ij}^n}{|\nabla f_{ij}^n|^n} = 0. \tag{3.31}$$

We denote the discriminant of quadratic equation (3.30) by

$$D = s_{ij}^2 |\nabla f_{ij}^n|^2 - 4d_{ij}^n \frac{(f_{ij}^n - G_{ij})}{|\nabla f_{ij}^n|^2}. \tag{3.32}$$

The second situation how to determine τ_{ij}^n is the situation when $D < 0$. In this case there exists no τ such that $\tilde{f}_{ij}^{n+1}(\tau) = G_{ij}$, therefore we need to control only the case 2 by requiring from (3.31)

$$\tau_{ij}^n = \min\left\{h, -\frac{s_{ij}|\nabla f_{ij}^n|^3}{2d_{ij}^n}\right\}. \tag{3.33}$$

Note that if $D < 0$ then $\text{sgn}(d_{ij}^n) = -s_{ij}$, so one has that $\tau_{ij}^n > 0$ in (3.33).

The third situation is given by $D > 0$. In this case there exists two values of τ such that $\tilde{f}_{ij}^{n+1}(\tau) = G_{ij}$, but only one root satisfies that $0 \leq \tau$. Using the standard formula for the roots of quadratic equation one can show that to control the case 1 one has to define

$$\tau_{ij}^n = \min\left\{h, \frac{s_{ij}|\nabla f_{ij}^n|^2 \left(\sqrt{D} - |\nabla f_{ij}^n|\right)}{2d_{ij}^n}\right\}. \tag{3.34}$$

Note that if $s_{ij}d_{ij}^n < 0$ then $\sqrt{D} < |\nabla f_{ij}^n|$ and if $s_{ij}d_{ij}^n > 0$ then $\sqrt{D} > |\nabla f_{ij}^n|$, so one has that $\tau_{ij}^n > 0$ in (3.34).

We can summarize that depending on the value of d_{ij}^n in (3.27) and D in (3.32) one can define the value of τ_{ij}^n by (3.29),(3.33), or (3.34) that can be used in (3.26) to define the values $\tilde{f}_{ij}^{n+1}(\tau_{ij}^n)$.

Having the value τ_{ij}^n the approximate characteristic curves $\tilde{X}_{ij}^{n,0}$ defined in (3.2) can be used to determine the new value f_{ij}^{n+1} by (3.3). When $n = N$ the optical flow $\vec{U}$ between F and G is given by (3.4).

4 Numerical experiment with exact solutions

We present here the results obtained by the Lucas and Kanade method and the method based on level set motion. This chapter includes the synthetic data for which we know the exact solutions.

We consider here a two dimensional distance function on a unit square, it means that $h = \frac{1}{I-1}$ for $I = J$. The image F is defined using the distance function (see Fig. 4) in the form

$$F_{ij} = \sqrt{(ih - s_x)^2 + (jh - s_y)^2}\,, \tag{4.1}$$

where (s_x, s_y) are the coordinates of the center of the unit square. We describe two numerical experiments - a movement of the distance function in the x direction and an expansion of the distance function.
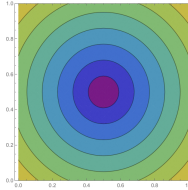

Figure 4: The distance function F_{ij}.

Once we determine the approximation of function f_{ij}^n using (3.3) we check the approximation quality of numerical method by comparing f_{ij}^n with the function G_{ij}. The difference function E^n is obtained by $E_{ij}^n = (G_{ij} - f_{ij}^n)$ and the norm of E_{ij}^n is calculated as follow

$$\|E^n\|_1 = h^2 \sum_{i,j \in \Omega} |E_{ij}^n|\,. \tag{4.2}$$

For the experiment we will known the exact deformation of optical flow that we denote by $\vec{V}_{ij} = (V_{ij}^1, V_{ij}^2)$. We compute the L^1-norm of the error for the deformation in x-direction $\|X\|_1$ as follows

$$\|X\|_1 = h^2 \sum_{i,j \in \Omega} |V_{ij}^1 - U_{ij}^1|\,. \tag{4.3}$$

and the L^1-norm of the error in the deformation in y-direction $\|Y\|_1$

$$\|Y\|_1 = h^2 \sum_{i,j \in \Omega} |V_{ij}^2 - U_{ij}^2|. \tag{4.4}$$

The optical flows are presented graphically as $-\vec{U}_{ij}$, resp. $-\vec{V}_{ij}$ using arrows, because we want to show that the position $\mathbf{x}_{ij}$ in the image G (where an arrow starts) comes from the image F in the position $\mathbf{x}_{ij} - \vec{U}_{ij}$ (where the arrow ends). In our numerical experiments the known deformation $-\vec{V}$ is presented by blue color and the obtained deformation $-\vec{U}$ by red color.

4.1 Expansion of the distance function

In this experiment an expansion of the distance function with known optical flow is considered, see Fig. 5. This example is chosen to test a correct behaviour of our method. The first image is given by the values F defined in (4.1). The second image G for some chosen speed $S \in R > 0$ of the expansion in normal direction is defined as follows

$$G_{ij} = \max \left\{ 0, \sqrt{(ih - s_x)^2 + (jh - s_y)^2} - S \right\}. \tag{4.5}$$

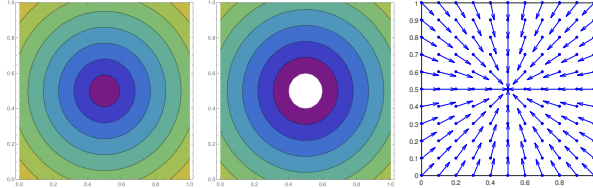The illustrative images of the expansion for $S = 0.1$ are shown in Fig. 5.

Figure 5: The expansion example. From the left to the right: the function F, the function G, the exact deformation $-\vec{V}$.

The expansion for this experiment is chosen such that $S = 0.1$. In this experiment we use the Lucas and Kanade method and the method based on level set motion. We aim to show an importance of the choice of convolution matrix for the Lucas and Kanade method on the approximation quality of numerical results. For the method based on level set motion we aim to show that the estimated deformation converges to the exact values. The results are shown in Fig. 6 - Fig. 9 for Lucas and Kanade method and in Fig. 10 - Fig. 11 for the method based on the level-set motion.

We begin with a discussion on the results obtained by Lucas and Kanade method. Firstly, we describe the influence of the choice of the convolution matrix for this method. We solve the problem with $I = J = 11$, i.e. $h = 0.1$ and $N = 2$ when the convolution matrices of dimensions $M = 3, 5, 7, 9, 11$ are used. The obtained deformations for the discrete convolution matrices 3×3, 7×7 and 11×11 are shown in Fig. 6 - Fig. 8(left).

The comparison of the obtained deformation $-\vec{U}$ with the known deformation $-\vec{V}$ are shown in Fig. 6 - Fig. 8(right). The L_1 norms defined in (4.2)-(4.4) is presented in Tab. 1.
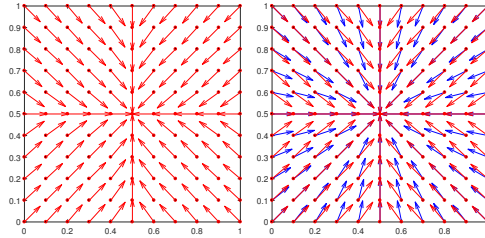

Figure 6: The results of expansion obtained by Lucas and Kanade method. From the left to the right: the deformation $-\vec{U}$ obtained using the convolution matrix 3×3, the comparison of the obtained optical flow $-\vec{U}$ (red) with the exact solution $-\vec{V}$ (blue).

Figure 7: The results of expansion obtained by Lucas and Kanade method. From the left to the right: the deformation $-\vec{U}$ obtained using the convolution matrix 7×7, the comparison of the obtained deformation $-\vec{U}$ (red) with the exact solution $-\vec{V}$ (blue).
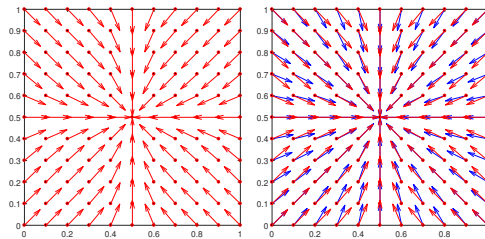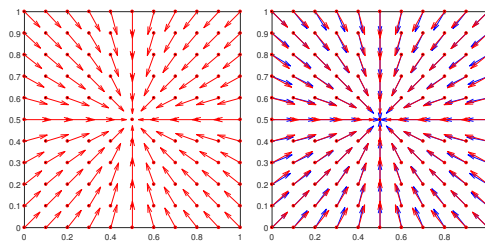

Figure 8: The results of expansion obtained by Lucas and Kanade method. From the left to the right: the deformation $-\vec{U}$ obtained using the convolution matrix 11×11, the comparison of the obtained deformation $-\vec{U}$ (red) with the exact solution $-\vec{V}$ (blue).

From the visual inspection of deformations in Fig. 6 - Fig. 8(right) we can see that the deformation obtained by the matrix 11×11 is much more accurate when compared

I	N	M	$\|E^N\|_1$	$\|X\|_1$	$\|Y\|_1$
11	2	3	0.002112	0.014650	0.014650
11	2	5	0.003449	0.013484	0.0,013484
11	2	7	0.004652	0.010969	0.010969
11	2	9	0.005852	0.009109	0.009109
11	2	11	0.006926	0.007085	0.007085

Table 1: The L_1-norms of expansion for Lucas and Kanade method for $I = 11$, $N = 2$ and $M = 3, 5, 7, 9, 11$.

with the results obtained by matrix 7×7 or 3×3. It can be seen not only from a visual inspection of the deformations in Fig. 6 - Fig. 8(right) but also from the norms in x-direction $\|X\|_1$ and y-direction $\|Y\|_1$ in Tab. 1. On the other hand with increasing the size of convolution matrix the norm of E^N is also increasing, see $\|E^N\|_1$ in Tab. 1. The first reason for such behaviour can be a worse quality of the approximation $\vec{U}$ in a neighbourhood of the center (s_x, s_y) where the assumption of locally constant deformation for the Lucas Kanade method is not so appropriate. Another reason might be that the values G_{ij} are obtained in (4.5) from the distance function F and not from the bilinear interpolation of values F_{ij}.

From this experiment we see that it needs not to be trivial to choose a proper size of the matrix for the convolution, because the results are quite sensitive to this choice.

Next, we discuss the results obtained by the Lucas and Kanade method and the method based on level set motion for different sizes of data. For both methods we consider the same sizes $I = J = 11, 21, 41, 81, 161$, i.e. $h = 0.1, 0.05, 0.025, 0.0125, 0.00625$. The number of steps N will be doubled for each I and we choose $N = 2, 4, 8, 16, 32$ for the Lucas and Kanade method and $N = 1, 2, 4, 8, 16$ for the method based on level set motion. The larger value of N for the Lucas Kanade method is motivated by more restrictive condition (3.15) on the time steps than the condition (3.25) given for the method based on level set motion.

For a better visualization of deformations, the deformations are presented for $I = J = 21, 41, 81$ using only the positions $\mathbf{x}_{ij}$ given by the coarsest grid with $I = J = 11$. The size of convolution matrices for Lucas and Kanade method is set to $M = 3, 5, 9, 17, 33$ for the increasing value of I. The results obtained by Lucas and Kanade method are shown in Fig. 9 and all L^1-norms are written in Tab. 2. From a visual inspection of deformations in Fig. 9 we can see that the deformation is more accurate with the refined grids. It can seen also from the L^1-norms in Tab. 2, but the rates of convergence for this example using the Lucas Kanade method is decreasing for the chosen parameters.
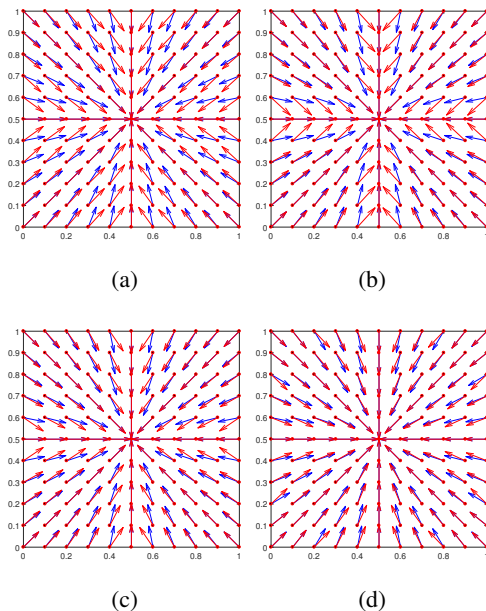
(a)

(b)

(c)

(d)

Figure 9: The results of expansion obtained by the Lucas and Kanade method. From the left to the right and from the top to the bottom: (a) the deformation $-\vec{U}$ obtained using $I = 11, N = 2$ and $M = 3$, (b) the deformation $-\vec{U}$ obtained using $I = 21, N = 4$ and $M = 5$, (c) the deformation $-\vec{U}$ obtained using $I = 41, N = 8$ and $M = 9$, (d) the deformation $-\vec{U}$ obtained using $I = 81, N = 16$ and $M = 17$.

I	N	M	$\|E^N\|_1$	rate	$\|X\|_1$	rate	$\|Y\|_1$	rate
11	2	3	0.002112	-	0.014650	-	0.014650	-
21	4	5	0.001042	1.01925	0.010397	0.494733	0.010397	0.494733
41	8	9	0.000583	0.837787	0.008118	0.356971	0.008118	0.356971
81	16	17	0.000345	0.756900	0.006641	0.289924	0.006641	0.289924
161	32	33	0.000292	0.240628	0.006489	0.0334043	0.006489	0.0334043

Table 2: The L_1-norms of expansion for deformation obtained by the Lucas and Kanade method for $S = 0.1$ and $I = 11, 21, 41, 81, 161$ and the rate of convergence.

The results obtained by the method based on level-set motion are shown in Fig. 10 for $I = 11$ and in Fig. 11 for $I = 11, 21, 41, 81$. From a visual inspection of deformations in Fig. 10 we can see that the estimated deformation is more accurate with the refined grids and we conclude that the results are satisfactory. For this method the rates of convergence for all norms, i.e. $\|E^N\|_1$, $\|X\|_1$ and $\|Y\|_1$, are approaching the value 1 as it can be seen in Tab. 3.
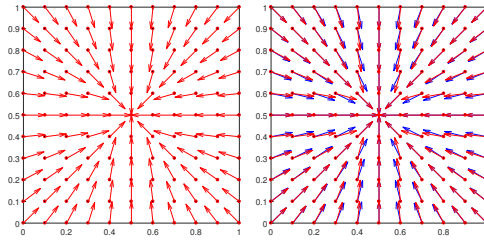
Figure 10: The result of expansion obtained by method based on level-set motion for expansion. From the left to the right: the obtained deformation $-\vec{U}_{ij}$, the comparison of the exact deformation (blue) and the obtained deformation (red).

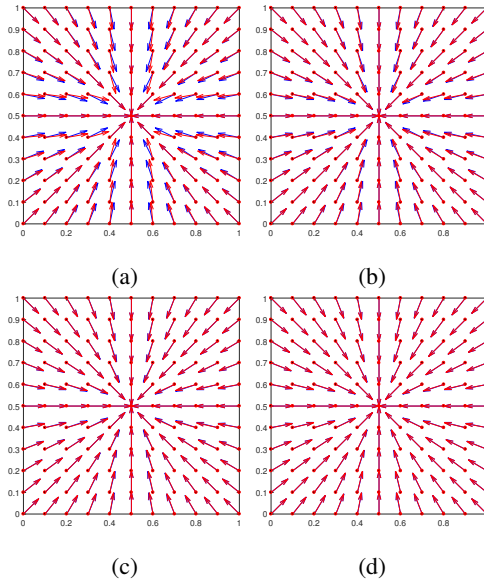(a)   (b)

(c)   (d)

Figure 11: The result of expansion example obtained by method based on level-set motion for expansion. From the left to the right and from the top to the bottom: (a) the deformation $-\vec{U}$ for $I = 11$, (b) the deformation $-\vec{U}$ for $I = 21$, (c) the deformation $-\vec{U}$ for $I = 41$, (d) the deformation $-\vec{U}$ for $I = 81$.

19

I	N	$\|E^N\|_1$	rate	$\|X\|_1$	rate	$\|Y\|_1$	rate
11	1	0.003120	-	0.004433	-	0.004433	-
21	2	0.001307	1.2556	0.002379	0.8985	0.002379	0.8985
41	4	0.000528	1.3075	0.001259	0.9175	0.001259	0.9175
81	8	0.000220	1.2667	0.000659	0.9339	0.000659	0.9339
161	16	0.000096	1.1947	0.000339	0.9590	0.000339	0.9590

Table 3: The L_1-norms of expansion for deformation obtained by method based on level-set motion for $S = 0.1$ and $I = 11, 21, 41, 81, 161$ and the rate of convergence.

5 Conclusions

In this work we present two numerical methods of optical flow estimation between two input functions. The both methods are based on the solution of advection equation that gives us the function evolving from the initial condition given by the first function towards the second function at some finite time.

The final optical flow is obtained sequentially for consecutive time steps. For each time step the advection equation is solved numerically where we suggest suitable numerical discretization for each method of the optical flow estimation. To find the deformation for the optical flow the backward tracking of characteristic curves for the advection equation is used in both methods. We describe the modification for the numerical tracking of characteristics that is less computationally demanding than the standard form of backward tracking method.

The two numerical methods for optical flow estimation differ in the approach which additional constraint is required for the velocity field in the advection equation.

The first method is based on the Lucas and Kanade method defined in [7]. This method assumes constant optical flow within some local neighborhood of each point in the computational domain. Using this assumption the additional constraint on the velocity field in the advection equation is obtained by the minimization of suitable functional where the convolution integral is involved. Our modification of this method introduces the CFL condition on the choice of time steps that enables us to apply the method also for large deformations to some extend.

The second method is based on level set motion and it is motivated by works of Sapiro et al. [1] and Vemuri et al. [12]. The additional constraint for $\vec{u}$ is obtained by restricting the optical flow only to normal directions to the level sets of the evolving function. We slightly modify the level set equation presented in [1, 12] by allowing the speed in normal direction having only three discrete values. Moreover we propose the new discretization method for the solution of advection equation for the motion in normal direction that is based on the more natural bilinear interpolation of the numerical solution. The modified formulation of the level set equation and the new discretization methods enables us to use less restrictive CFL condition for the choice of time steps and apply it for the functions representing images for which the bilinear interpolation is used typically.

References

[1] M. BARTALMÍO, G. SAPIRO, G. RANDALL, *Morphing Active Contours.*, IEEE Trans. PAMI, 22(7) (2000), pp. 733-737.

[2] J. Y. BOUGUET, *Pyramidal Implementation of the Lucas-Kanade Feature Tracker.*, Tech. Rep., Intel Corporation, Microprocessor Research Labs, (1999).

[3] A. BRUHN, J. WEICKERT, CH. SCHNÖRR, *Lucas/Kanade Meets Horn/Schunck: Combining Local and Global Optic Flow Methods.*, Int. Journal of Comp. Vision , 61(3) (2005), pp. 211-231.

[4] P. COLELLA, *Multidimensional upwind methods for hyperbolic conservation laws.*, J. Comput. Phys. , 87(1) (1990), pp. 171-200.

[5] F. GIBOU, R. FEDKIW, S. OSHER, *A review of level-set methods and some recent applications.*, J. Comput. Phys. , 353 (2017), pp. 82-109.

[6] B. HORN, B. SCHUNCK, *Determining optic flow.*, Artificial Intelligence, 17(1-3) (1981), pp. 185-203.

[7] B. LUCAS, T. KANADE, *An iterative image registration technique with an application to stereovision.*, In Int. Joint Conf. on Artificial Intel, 2 (1981), pp. 674-679.

[8] S. OSHER, J.A. SETHIAN, *Fronts Propagating with Curvature Dependent Speed: Algorithms Based on Hamilton-Jacobi Formulations* , J. Computational Physics, 79 (1988), pp. 12-49.

[9] J.A. SETHIAN, *Level Set Methods and Fast Marching Methods*, Cambridge University Press, 2 (1999), ISBN: 9780521645577.

[10] RANDALL J. LEVEQUE, *Finite Volume Methods for Hyperbolic Problems.*, Cambridge University Press, 1 (2002), ISBN: 0521009243.

[11] E. ROUY, A. TOURIN, *A viscosity solutions approach to shape-from-shading.*, SIAM J. Num. Anal., 29 (1992), pp. 867-884.

[12] B.C. VEMURI, J. YE, Y. CHEN, C.M. LEONARD, *Image registration via level-set motion: Applications to atlas-based segmentation.*, Medical Image Analysis, 7(1) (2003), pp. 1-20.

The author's publications

- P. FROLKOVIČ, V. KLEINOVÁ, *Two methods for optical flow estimation..*, In Proceedings of Equadiff 2017 Conference [elektronický zdroj] : July 24-28, 2017, Bratislava, Slovakia. 1. vyd. Bratislava : Spektrum STU, online, ISBN 978-80-227-4757-8. V databáze: WOS: 000426796700038., (2017) pp. 331-340.

- V. KLEINOVÁ, P. FROLKOVIČ, *Numerical solution of advection equation for the motion in normal direction with application in optical flow estimation.*, In Advances in Architectural, Civil and Environmental Engineering [elektronický zdroj] : 27th Annual PhD Student Conference on Applied Mathematics, Applied Mechanics, Geodesy and Cartography, Landscaping, Building Technology, Theory and Structures of Buildings, Theory and Structures of Civil Engineering Works, Theory and Environmental Technology of Buildings, Water Resources Engineering. 25. October 2017, Bratislava, Slovakia. 1. vyd. Bratislava : Spektrum STU, CD-ROM, ISBN 978-80-227-4751-6, (2017), pp. 28-34.

- V. KLEINOVÁ, *Backward tracking method in optical flow.*, In Advances in Architectural, Civil and Environmental Engineering [elektronický zdroj] : 26th Annual PhD Student Conference on Architecture and Construction Engineering, Building Materials, Structural Engineering, Water and Environmental Engineering, Transportation Engineering, Surveying, Geodesy, and Applied Mathematics. 26. October 2016, Bratislava. 1. vyd. Bratislava : Slovenská technická univerzita v Bratislave, CD-ROM, ISBN 978-80-227-4645-8, (2016), pp. 38-43.

- V. KLEINOVÁ, *Algorithms to compute the optic flow in image processing and their comparison.*, In Advances in architectural, civil and environmental engineering [elektronický zdroj] : 25rd Annual PhD Student Conference on Architecture and Construction Engineering, Building Materials, Structural Engineering, Water and Environmental Engineering, Transportation Engineering, Surveying, Geodesy, and Applied Mathematics. Bratislava, SR, 28. 10. 2015. 1. vyd. Bratislava : Slovenská technická univerzita v Bratislave, CD-ROM, ISBN 978-80-227-4514-7, (2015), pp. 44-50.